Preparation of nano SnO$_2$-Sb$_2$O$_3$ composite electrode by cathodic deposition for the elimination of phenol by Sonoelectrochemical oxidation

Hind Jabbar Nsaif[1], Najwa Saber Majeed[1], Rasha H. Salman[1*]

Department of Chemical Engineering, College of Engineering, University of Baghdad, Baghdad, Iraq
*Corresponding author: e-mail: rasha.habeeb@coeng.uobaghdad.edu.iq

The preparation of composite metal oxide to attain high efficiency in removing phenol from wastewater has a great concern. In the present study, the focus would be on adopting antimony-tin oxide coating onto graphite substrates instead of titanium; besides the effect of SbCl$_3$ concentration on the SnO$_2$-Sb$_2$O$_3$ composite would be examined. The performance of this composite electrode as the working electrode in the removal of phenol by sonoelectrochemical oxidation will be studied. The antimony-tin dioxide composite electrode was prepared by cathodic deposition with SnCl$_2$. 2H$_2$O solution in a mixture of HNO$_3$ and NaNO$_3$, with different concentrations of SbCl$_3$. The SnO$_2$-Sb$_2$O$_3$ deposit layer's structure and morphology were examined and the 4 g/l SbCl$_3$ gave the more crystallized with nanoscale electrodeposition. The highest removal of phenol was 100% at a temperature of 30 °C, with a current density (CD) of 25 mA/cm^2.

Keywords: antimony-tin oxide, electrodeposition, sonoelectrochemical, phenol, nano composite.

INTRODUCTION

Recent releases of wastewater from industries that contain hazardous and non-degradable organic chemicals into the aquatic environment have major concern [1]. Phenol is one of the particularly dangerous organic contaminants found in wastewater. Due to their significant toxicity to humans, aquatic life, and the environment even at low concentrations, phenols were categorized as a priority contaminant[2–5].
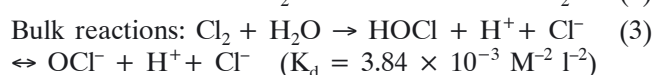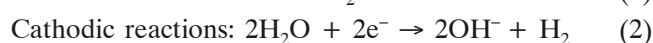
For the removal of phenol, both conventional and modern methods have been used, including microbial degradation[6], extraction[7], electro-coagulation[8], electro-Fenton technique[9], photo-decomposition[10], ion exchange[11], adsorption[12], and Advanced Oxidation Process (AOP)[13].

AOP processes, such as chemical oxidation, electrochemical oxidation, photocatalytic oxidation, and sonochemical oxidation, have received a lot of attention due to the variety, quantity, and complexity of nonbiodegradable pollutants. Each technique has distinct benefits, but in some circumstances, it can be challenging for a single oxidation method to provide the requirements for wastewater treatment. However, combining several oxidation processes has emerged as one of the potential options and active research areas. In the last years, ultrasound and an electrochemical reaction have been combined in sonoelectrochemistry[14].

Sonoelectrochemistry process can rapidly decompose organic contaminants in wastewater producing water, carbon dioxide, inorganic ions, and another significant benefit of sonoelectrochemistry is that it can be performed in accepting conditions with high micromixing and cleaning the surface of the electrode by dissolving the inhibitory layers, which increases the mass transfer between the solid and liquid[15].

The cavitation (bubbles formation and deflation) that is generated by intense ultrasound enables the possibility for decomposition of organic compounds in wastewater. The formed bubble expands throughout the rarefaction stage and collapses throughout the compression stage, and as a result of quasi-adiabatic collapse, the temperature inside the bubble becomes very high[16], As a result, oxygen and water vapor, if available, have dissociated leading to the formation of oxidants like OH$^•$, and H$_2$O$_2$[17, 18].

Electrochemical Oxidation of toxic pollutants in wastewater can be attained by two types of oxidations direct and indirect. In the direct electrochemical oxidation method, organic compounds oxidized by OH$^•$ radicals, while in the indirect oxidation, the pollutants have been destroyed by the action of active chlorine and hypochlorite produced at the anode[19]. Equations (1–3) show the important chemical reaction at the anode, cathode, and bulk during the indirect electrochemical process[20, 21].

Anodic reactions: $2Cl^- \rightarrow Cl_2 + 2e^-$ (1)

Cathodic reactions: $2H_2O + 2e^- \rightarrow 2OH^- + H_2$ (2)

Bulk reactions: $Cl_2 + H_2O \rightarrow HOCl + H^+ + Cl^-$ (3)
$\leftrightarrow OCl^- + H^+ + Cl^-$ $(K_d = 3.84 \times 10^{-3} \, M^{-2} \, l^{-2})$

The performance and efficiency of electrochemical processes are affected by several factors, including electrode potential and electrode materials. The best degradation of phenol can be obtained when the electrode material has a high oxygen overpotential, excellent electrical conductivity, and high stability[15, 22].

Several kinds of electrode materials like RuO$_2$[23], IrO$_2$[24], boron-doped diamond (BDD)[25], PbO$_2$[26], and SnO$_2$[27] have been investigated. Due to their scientific importance and the possibility of applications, mixed oxides of metal on metal substrates have the interest of many researchers[28].

Several chemical elements, including Sb, B, Ar, F, B, Cl, and P, have been utilized as dopants, but Sb is the most successful in boosting the electrocatalytic activity because of their high oxygen evolution overpotential and ability to produce hydroxyl radicals quickly, Sb-doped SnO$_2$ anodes are known to facilitate the indirect oxidation of organic contaminants[22]. Sb$_2$O$_3$ was added to strengthen the active catalytic layer of SnO$_2$. Besides, Sb$_2$O$_3$ enhanced the breakdown of phenol organics, implying that it should contribute to SnO$_2$ catalysis[29]. In comparison with various electrodes, SnO$_2$ –Sb$_2$O$_3$ electrodes are well-known as having high oxygen-evolution overpotential and highly effective for the generation of OH, so it has high performance for the oxidation of organic compounds[30–32].

According to some results, the effectiveness of anodes is primarily connected to the structure and particle size of the SnO$_2$ coating on base materials. As the crystal size of the coating is reduced to a nanometer, nanoscale

materials exhibit extraordinary physical and chemical properties that differ from conventional materials because of the quantum effect, tiny size effect, surface effect, and tunneling effect[33]. As a result, SnO_2-Sb_2O_3 nanocoating may have better electrocatalytic efficiency.

In this work, tin-antimony oxide film electrode was prepared by using cathodic electrodeposition on graphite substrate followed by thermal oxidation and studying the effect of the concentrations of $SnCl_2 \cdot 2H_2O$ and $SbCl_3$ on the electrode's structure and morphology. The performance of the prepared electrode was then tested in the sonoelectrochemical process for phenol removal; these tests were carried out at various temperatures, Current densities, and phenol concentrations.

EXPERIMENTAL WORK

Chemicals

All chemicals were employed in the reagent-grade, no additional purification was necessary, $SnCl_2 \cdot 2H_2O$ (Thomas Baker), $SbCl_3$ (Merck, Darmstadt, Germany), H_2SO_4 (Alpha Chemika), $NaNO_3$ (Alpha Chemika), phenol (LOBA Chemie), HNO_3 (Alpha Chemika), NaCl (Central Drug House (P) Ltd -CDH), HNO_3 (Alpha Chemika), and all aqueous solutions were produced using deionized water.

Preparation of SnO_2-Sb_2O_3 anode

A tin oxide electrode was prepared by our previous study[34], but in the current study, the electrode was improved by preparing a composite of SnO_2 with Sb_2O_3 to enhance its properties. There is no previous study that used this composite in the sonoelectrochemical oxidation process. The tin-antimony oxide composite electrode was prepared by the cathodic electrodeposition method. Two graphite substrate plates of) 6.5 cm × 8 cm (were firstly polished by 2000-grit paper and using water as a lubricant, cleaned by ultrasonic for 10 min, washed with ethanol, and then boiled in deionized water for 30 min. After that, electrochemically activated in 1.44 M of H_2SO_4 electrolyte by applying CD equal to 14 mA/cm² at 90 ºC for 30 minutes, a magnetic stirrer (Nahita Blue; model 692/1) was employed to heat this electrolyte, and then the electrode was washed by using deionized water. The cathodic deposition was carried out in solutions of 50 and 75 mM $SnCl_2 \cdot 2H_2O$, 100 mM $NaNO_3$[35] and 250 mM HNO_3. The solutions were stirred for 3 h at 85 ºC to convert Sn^{2+} into Sn^{4+} ions, after this, a specified amount of $SbCl_3$ (1, 2, or 4 g/l) were added to the solution. The prepared graphite was immersed in this electrolytic solution with a 2.5 cm gap between the anode and cathode. The constant CD of 10 mA/cm² was supplied by a power supply (Maisheng, MS-605D), and a current multimeter was used to measure the applied current. The electrodeposition process was accomplished within 1 h and the temperature was maintained at 85 °C, and the time 1 h, then the electrode was calcined at 600 ºC for 2 h[31].
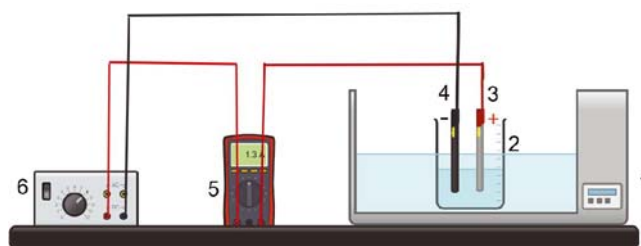
Sonoelectrochemical Process

The performance of SnO_2–Sb_2O_3 electrode was examined by using it to remove chemical oxygen demand (COD) from simulated wastewater with 150 mg/l of phenol, with 3g/l of NaCl (as the supporting electrolyte), and a few drops of H_2SO_4 (to make the pH of wastewater equal to 3) the electrolytic solution was mixed with 250 rpm. The electrochemical cell, a Glass beaker with 500 ml volume, was placed in an ultrasonic bath (Ultrasonic; model: 031S) at a frequency equal to 40 kHz[17] as shown in Figure 1. The prepared electrode was used as an anode and a graphite plate as a cathode and the distance between them was 2.5 cm. DC power supply was employed to supply the adequate current. The performance of the sonoelectrochemical oxidation was evaluated by determining the chemical oxygen demand (because phenol is transformed into other organic molecules, it is preferable to estimate the COD) by using a COD reactor (Lovibond; RD125), after that the sample was analyzed by spectro-photometer (Lovibond Water Testing; MD 200 COD; Germany), COD removal efficiency was determined as follows[36, 37].

$$\text{COD removal } \% = \frac{COD_o - COD_f}{COD_o} \times 100\% \qquad (4)$$

Where: COD_o and COD_f are the initial and final values of COD in mg/l.

Figure 1. Scheme diagram of the sonoelectrochemical process, 1. Digital ultrasonic bath, 2. Beaker, 3. SnO_2 anode, 4. Graphite cathode, 5. Multimeter, and 6. Power supply

RESULTS AND DISCUSSION

The majority of the studies on tin oxide electrodes have focused on the influence of doping concentration on SnO_2 conductivity[38, 39], but no author has reported on the effect of $SbCl_3$ concentration on SnO_2-Sb_2O_3 electrode organic degrading activity, the current study shows that Sb_2O_3 is an important factor in organic removal.

The X-ray diffraction (XRD) Results

The XRD was employed to detect the crystalline structures of Sn and Sb oxides deposited on cathodes in the range (5–80º) of 2θ, and the results are given in Figure 2. The XRD peaks of SnO_2 electrode (Figure 2A) were assigned at 2θ values of 26.78º, 34.01º, 38.09º, 52.06º, and 54.23º which are related to the lattices of (110), (101), (200), (211), and (220) respectively. These peaks all accord quite well with the data for tetragonal SnO_2 (JCPDS no. 41-1445). The XRD peaks of the SnO_2- Sb_2O_3 electrode with 1 g/l of $SbCl_3$ (as shown in Figure 2 B) at 26.61°, 34.13°, 38.13°, 52.32°, and 54.66° corresponded to the (110), (101), (200), (211), and (220) planes of the tetragonal SnO_2. However, the peaks at 28.70°, 34.13°, and 54.66° corresponded to the (121), (012), and (170) planes of the orthorhombic valentinite phase of Sb_2O_3 (JCPDS File No. 11-0689).
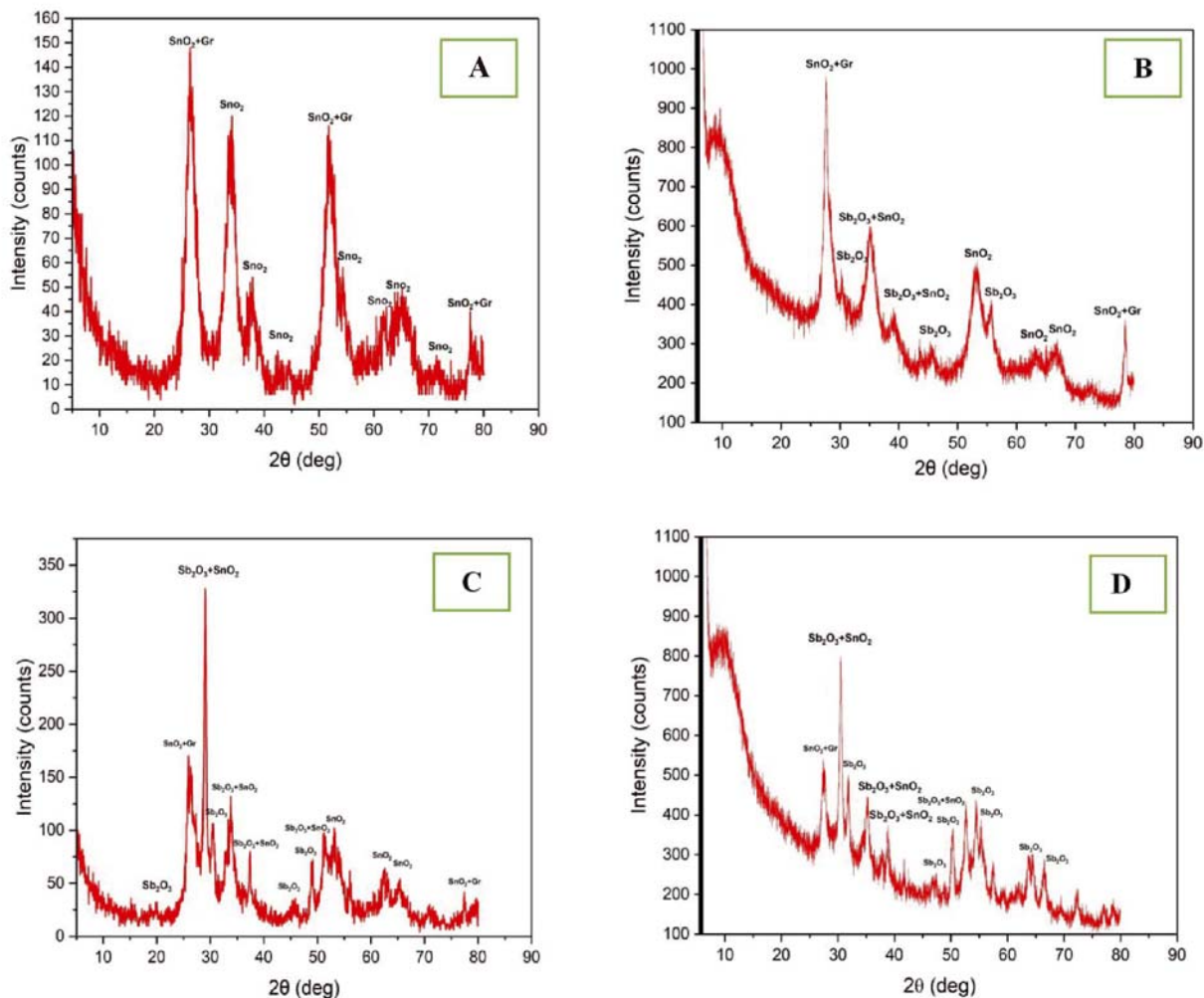
Figure 2. XRD of (A) SnO$_2$ electrode, (B-C) SnO$_2$-Sb$_2$O$_3$ electrodes, prepared by addition, B= 1, C= 2, and D= 4 g/l SbCl$_3$ concentration

For the SnO$_2$-Sb$_2$O$_3$ electrode with 2 g/l SbCl$_3$, XRD peaks (Figure 2C) at 26.35°, 33.88°, 37.37°, and 51.027° fit the tetragonal SnO$_2$ planes (110), (101), (200), and (211). However, the peaks at 29.07°, 33.88°, 37.37°, and 50.58° corresponded to the (121), (012), (200), and (161) planes of the orthorhombic valentinite phase of Sb$_2$O$_3$. Figure 2D shows the XRD peaks of SnO$_2$- Sb$_2$O$_3$ electrode with 4g/l of SbCl$_3$ at 26.59°, 34.16°, 37.78°, 51.60°, and 54.4727° fit the (110), (101), (200), and (211), and a (220) planes of the tetragonal SnO$_2$. The peaks at 29.47°, 34.16°, 36.69°, 50.25°, and 54.47° referred to the orthorhombic valentinite phase of Sb$_2$O$_3$ planes (121), (012), (200), and (161), and (170). This demonstrated that the graphite surface was predominantly loaded with Sn-Sb oxides[40, 41]

The Scherrer equation was used to compute the crystal size[42].

$$D = 0.8 \, \lambda \, / \, \beta \, Cos \, \theta \qquad (5)$$

Table 1. Crystal sizes of prepared electrodes

Electrode type	crystal size, nm	
	SnO$_2$	Sb$_2$O$_3$
SnO$_2$	3.79	–
SnO$_2$-Sb$_2$O$_3$, (1 g/l SbCl$_3$)	7.735	5.5
SnO$_2$-Sb$_2$O$_3$, (2 g/l SbCl$_3$)	6.37	10.407
SnO$_2$-Sb$_2$O$_3$, (4 g/l SbCl$_3$)	12.059	13.49

Where λ = 0.15406 nm, β the full width at half maximum intensity (FWHM), and θ is the angle of Bragg diffraction. As shown in Table 1 the crystal size of the deposited materials increased with the increase of the SbCl$_3$ concentration due to the increase in the crystal lattice

The field-emission scanning electron microscopy (FE-SEM) and energy-dispersive X-ray spectroscopy (EDX) Results

Figure 3A depicts the SEM images of the SnO$_2$ electrode. Irregular spherical grains can be detected on the graphite substrate. As the nanocrystals coalesce, large crystallites form, and a porous morphology is created by organizing the crystals in a haphazard, non-uniform manner, these results agree with[22].

Figure 3(B-D) shows that the SEM images of the SnO$_2$-Sb$_2$O$_3$ electrodes which are changed noticeably as the SbCl$_3$ concentration changed. The films are formed from a network of nanoparticles with spherical morphology. It is apparent that the surface of the electrode is quite rough, with irregular pores, which has a greater specific surface area than the graphite substrate, this result agrees with[43].

Figure 3D shows the morphology of the SnO$_2$-Sb$_2$O$_3$ electrode with 4 g/l SbCl$_3$. The surface presents a uniform distribution of particles which is more granulated and

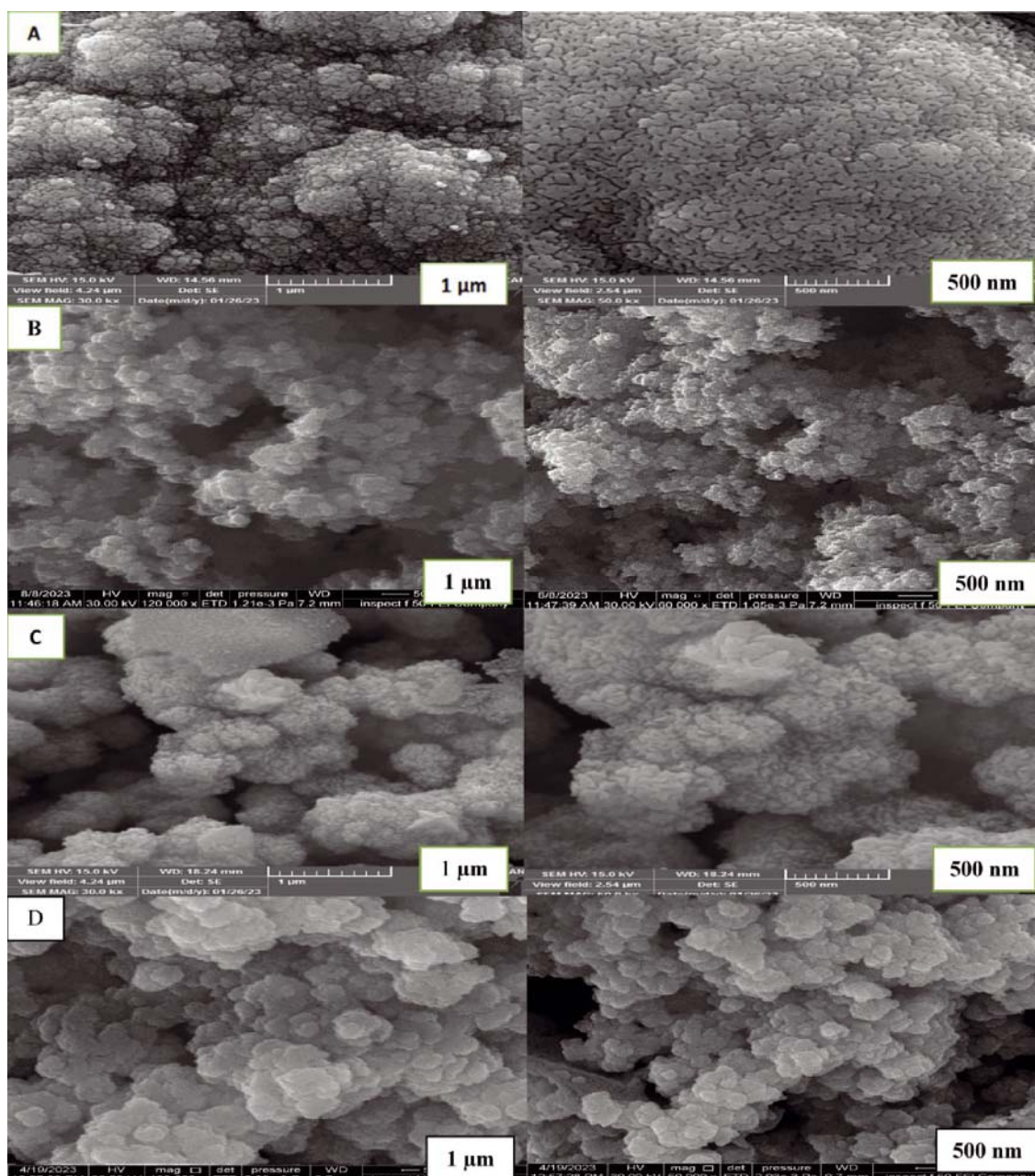**Table 2.** EDX of SnO$_2$ electrode, SnO$_2$-Sb$_2$O$_3$ electrodes, prepared by 1, 2, 4 g/l of SbCl$_3$

| Element | SnO$_2$ electrode | | SnO$_2$-Sb$_2$O$_3$ electrode | | | | | |
| | | | 1 g/l of SbCl$_3$ | | 2 g/l of SbCl$_3$ | | 4 g/l of SbCl$_3$ | |
	A%	Wt. %	A%	Wt. %	A%	Wt. %	A%	Wt. %
C	17.39	5.27	25.29	9.45	27.59	9.51	27.44	10.83
O	61.95	27.14	58.24	29.04	53.67	24.63	57.85	30.36
Sn	20.66	67.14	9.75	35.88	9.97	33.94	2.97	11.67
Sb	0	0	6.72	25.63	8.77	31.92	11.74	47.14
Total	100.00	100.00	100.00	100.00	100.00	100.00	100.00	100.00

spongy than that obtained for other electrodes and has a substantial quantity of graphite surface coverage[43]. The element composition of the electrodes was determined with EDX as shown in Table 2. In accordance with the atomic (A%) and weight (wt. %) percentages, the observed presence of Sn, Sb, and oxygen components in the EDX data implies that SnO$_2$ and Sb$_2$O$_3$ were successfully deposited on the graphite surface, and the results also showed that the components (Sn and Sb) are distributed uniformly on the electrode and a low amount of carbon was detected, indicating that Sn-Sb oxides covered the majority of the graphite surface. The Sb content was higher than anticipated, which might be because antimony made up the last layer, this result agrees with[32, 43, 44].

Atomic force microscopy (AFM) Results

Based on the results of XRD and SEM it could be revealed that the best electrode of SnO$_2$-Sb$_2$O$_3$ composite was attained with the 4 g/l of SbCl$_3$ concentration, where it could be concluded that this electrode gave the best crystallization and full coverage with Sn-Sb oxide, and its surface presents a uniform distribution of particles, which is more granulated than that obtained with other

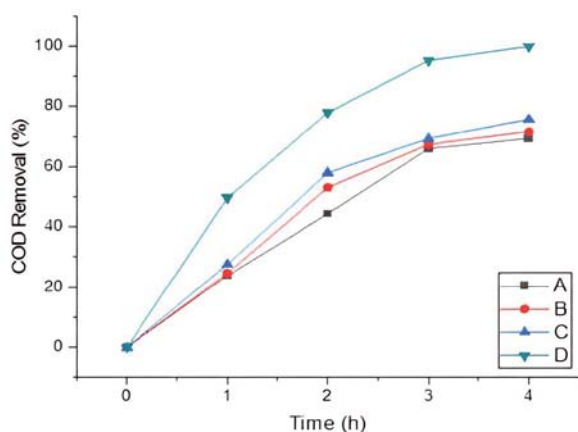**Figure 3.** SEM of (A) SnO$_2$ electrode, (B-D) SnO$_2$-Sb$_2$O$_3$ electrodes, prepared by add B=1, C=2, and D= 4 g/l SbCl$_3$ concentration
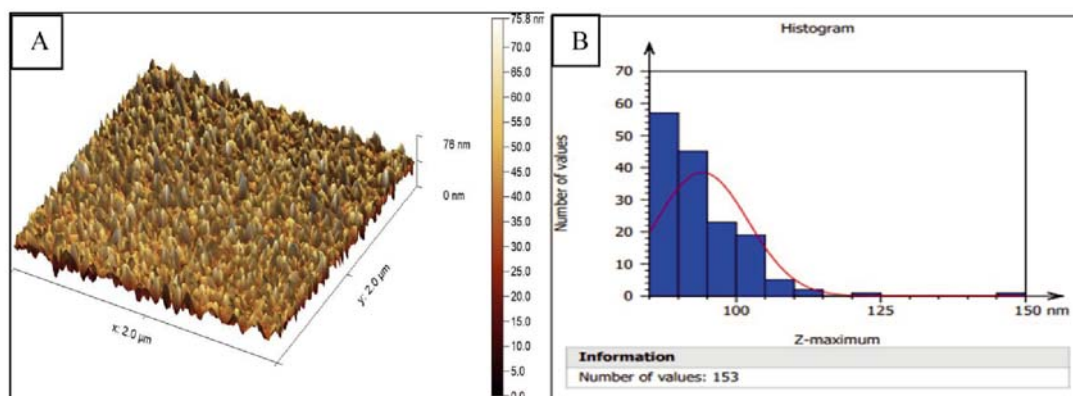
Figure 4. (A) AFM image of SnO$_2$-Sb$_2$O$_3$ surface, (B) Granularity Distribution

conditions. Structural and morphological analysis for this electrode was conducted with an Atomic Force Microscope (AFM) as shown in Figure 4. The average roughness of the film was 7.22720 nm. The statistical summary of SnO$_2$- Sb$_2$O$_3$ nanocomposite film on graphite illustrates that the mean particle diameter was 94.15 nm, the minimum particle diameter was 86.79 nm and the maximum particle diameter was 149.0 nm.

COD Removal with Sonoelectrochemical Process

Primary tests for COD removal were carried out by using graphite as the cathode and prepared SnO$_2$ electrode or SnO$_2$-Sb$_2$O$_3$ electrode with different concentrations of SbCl$_3$ as the anode in the sonoelectrochemical process have been carried out at initial phenol concentration of 150 mg/l, CD of 25 mA/cm^2, temperature of 30 °C, pH of 3, NaCl concentration of 3 g/l, and ultrasonic frequency of 40 kHz, Figure 5 shows that COD removal % was 69.33, 71.59, 75.79, and 100% for SnO$_2$ electrode, SnO$_2$-Sb$_2$O$_3$ electrode with 1 g/l, SnO$_2$-Sb$_2$O$_3$ electrode with 2 g/l, and SnO$_2$-Sb$_2$O$_3$ electrode with 4 g/l SbCl$_3$ concentration, respectively. This means that the best COD removal was obtained with SnO$_2$-Sb$_2$O$_3$ nanocomposite electrode with 4 g/l of SbCl$_3$, and the lower removal was obtained with SnO$_2$ electrode. This revealed that Sb$_2$O$_3$ is an important factor in the electrocatalytic activity of SnO$_2$-Sb$_2$O$_3$ electrodes because of its high activity in
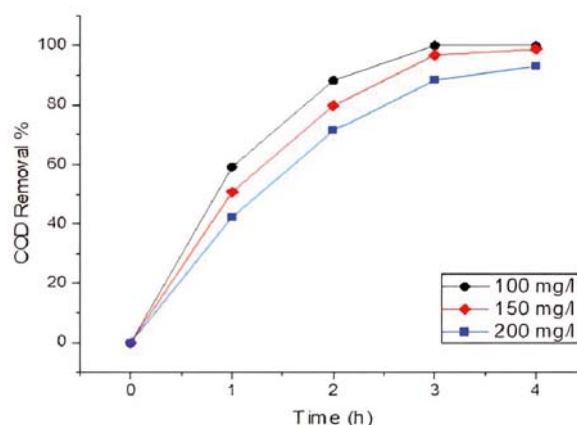
producing hydroxyl radicals. Hence the maximum removal of COD was attained with SnO$_2$-Sb$_2$O$_3$ nanocomposite electrode prepared with the addition of 4 g/l of SbCl$_3$; this electrode would be the anode in further investigation.

Effect of different parameters on COD removal

Effect of phenol concentration

To investigate the treatment efficiency with different initial concentrations of phenol, the experiments of sonoelectrochemical oxidation of 100, 150, and 200 mg/l phenol have been carried out at a current density of 25 mA/cm^2, temperature of 30 °C, pH of 3, NaCl concentration of 3 g/l, and ultrasonic frequency was 40 kHz. Figure 6 presents the experimental results where it is illustrated that the COD removal was 100% in 3 hours, for initial concentrations of phenol of 100 mg/l, 98.78% of COD was removed in 4 hours for 150 mg/l of phenol, and 93% of COD was removed in 4 hours, with 200 mg/l of phenol. Therefore, lower initial concentrations of phenol were associated with higher COD removal. In this case, the oxidants generated are adequate to completely oxidize the phenol. Furthermore, since the amount of oxidants created during the sonoelectrochemical oxidation process is constant under otherwise identical conditions, it is evident that the formed oxidants are insufficient to completely oxidize higher amounts of phenol. As a result, longer times were required for a higher initial concentration of phenol contaminants

Figure 5. COD removal at different electrodes, (A) SnO$_2$ electrode, (B-D) SnO$_2$-Sb$_2$O$_3$ electrodes, prepared by addition of B=1, C=2, and D= 4 g/l of SbCl$_3$, CD= 25 mA/cm2, temperature = 25 °C, NaCl conc.= 3 g/l, pH = 3, and 40 kHz ultrasonic frequency
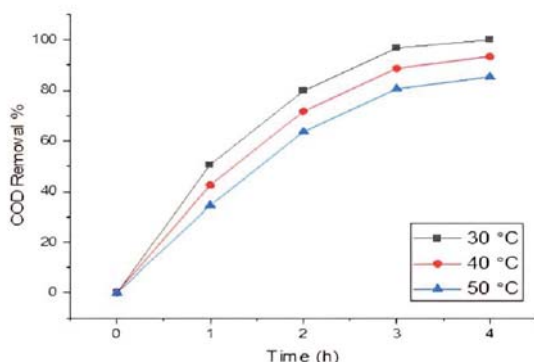

Figure 6. The effect of initial concentration of phenol on COD Removal %, at CD= 25 mA/cm^2, Temp. = 30 °C, pH = 3, NaCl conc. = 3 g/l, and Ultrasonic frequency = 40 kHz

to complete the oxidation process, and the electrolysis time needed for the complete removal of phenol was proportionate to its initial concentration[45–47].

Effect of temperature

In ultrasonic irradiation, the temperature of the reaction system is a more essential parameter because, during the sonoelectrochemical process, the temperature in the ultrasonicator rises. As a result, cooling the reactor is required to keep a constant temperature. Temperature's influence on the efficiency of sonoelectrochemical oxidation processes has not been thoroughly investigated[48]. This study investigated the effect of temperature on the process of COD removal from simulated wastewater by sonoelectrochemical.

The effect of temperature on COD removal is shown in Figure 7, The COD removal decreased from 100, 93.43, and 85.36 when the temperature increased from 30 to 40, and 50 °C, respectively. It can be noted that the increase the temperature causes a decrease in the amount of COD removed. The prevailing belief is that rising temperatures will increase the reactivity rates of contaminants with reactive oxidizing species, but the temperature of a solution affects the physicochemical properties of the solution such as vapor pressure and liquid viscosity, which has a direct impact on the cavitation process[49]. Higher operating temperatures increasing the solution's vapor pressure while decreasing its viscosity, allowing for the formation of additional cavitation bubbles. But the bubble collapse for cavitation is less strong, so less hydroxyl radical generation would be resulted[50]. Furthermore, the existence of too many bubbles may disturb the dispersion of ultrasonic power throughout the solution. This could explain why there were conflicting reports on the effect of temperature on the sonoelectrochemical process.

Figure 7. The effect of temperatures on COD removal, at CD = 25 mA/cm², Temp. = 30 °C, pH = 3, NaCl conc.= 3 g/l, initial concentrations of phenol = 150, and Ultrasonic frequency = 40 kHz

These results are consistent with the results of[51, 52] where they concluded that the maximum activity occurred at 35 °C.

Determining the complete effects caused by temperature on cavitation is very difficult, as this is mostly complicated by the effect of other interdependent variables such as the ultrasonic intensity, the number of bubbles produced, and so on. In addition, temperature is likely to affect the stability of the electrodes. High temperatures, for example, could cause the dissolution of metal oxide layers on the electrode[14].

Effect of current density

Previous studies have demonstrated that CD plays a significant role in the electrochemical process and that a higher CD is favorable to the combined system[47]. The sonoelectrochemical process was investigated with different CD (10, 20, and 25 mA/cm²) with a temperature of 30 °C, phenol concentration of 150 mg/l, pH of 3, NaCl concentration of 3 g/l, and the ultrasonic frequency was 40 kHz. The findings of COD removal were recorded for up to 4 hours as shown in Figure 8. The COD removal was increased from 73.54 to 82.228 and 100% when the CD increased from 10 to 20 and 25 mA/cm², respectively. The result indicates that phenol degradation increased by rising CD, and this attained as a result of the electrolysis producing more hydroxyl radical (OH•). These results agree with previous research findings of[53, 54].
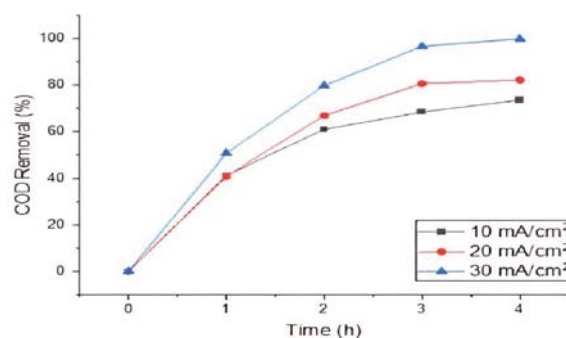
Figure 8. The Effect of CD on COD Removal, at Temp. = 30 °C, pH = 3, NaCl conc.= 3 g/l, initial concentrations of phenol= 150 mg/l, and Ultrasonic frequency = 40 kHz

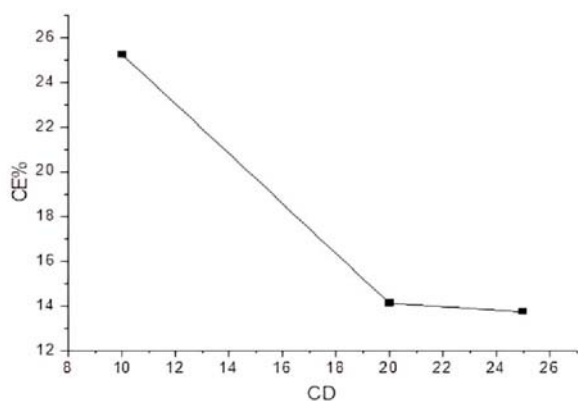### The Effect of the Current Density on the Current Efficiency

The most widely utilized energy measure for comparing and evaluating electrochemical treatment methods is current efficiency (CE), the CE is the percentage of the total current that is passed for the goal reaction in any electro-oxidation process, The CE aids in the comprehension and interpretation of the shift in the electrochemical treatment process's oxidative capability. From Equation 6, the CE% can be calculated as follows[55].

$$CE\% = \frac{F.V.\Delta COD}{8.I.t} \qquad (6)$$

Where F symbolizes the Faraday constant (96485.33 C/mol), V denotes the effluent volume in (L), ΔCOD represents the difference in the COD values in (g/L), I is the applied current in (A), 8 indicates a dimensional factor for unit consistency which is equivalent to the mass of oxygen (32 g of O_2 /4 mol of electrons) (g/mol), and t is the time of electrolysis (s).

CE % was calculated for COD removal in Sonoelectrochemical oxidation that resulted at various current densities, Temp. = 30 °C, pH = 3, NaCl conc. = 3 g/l, initial concentrations of phenol = 150 mg/l, and Ultrasonic frequency = 40 kHz to evaluate its effectiveness with SnO_2-Sb_2O_3 composite electrode.

Figure 9 shows that the lowest value of CD (10 mA/cm²) gave the highest value of CE% at 25.27 %.

Figure 9. The effect of the current density on the CE for COD Removal, at Temp. = 30 °C, pH = 3, NaCl conc.= 3 g/l, initial concentrations of phenol = 150 mg/l, and Ultrasonic frequency = 40 kHz

As CD increases the CE % decreases and the cause is the formation of intermediates. Our results concur with previous researches[56, 57].

CONCLUSIONS

A SnO$_2$ and SnO$_2$-Sb$_2$O$_3$ nanocomposite electrode were successfully prepared by using cathodic electrodeposition method; the result showed that Sb$_2$O$_3$ concentration is an important factor in the electrocatalytic activity of SnO$_2$-Sb$_2$O$_3$ nanocomposite electrodes. The highest removal of COD was obtained with SnO$_2$- Sb$_2$O$_3$ nanocomposite electrode with 4 g/l SbCl$_3$ concentration. The sonoelectrochemical indirect oxidation by using the SnO$_2$- Sb$_2$O$_3$ nanocomposite electrode is a promising technique for eliminating of organic pollutants from wastewater. The performance of the sonoelectrochemical removal of organic compounds is most affected by CD, phenol concentration, and temperature. As the initial phenol concentration increased from 100 to 200 mg/l, the COD removal % decreased from 100% at 3 hours to 93% at 4 hours, respectively. Increasing temperature had caused a decrease in the COD removal %. As the CD increased from 10 to 25 mA/cm^2, COD removal % increased from 73.54 to 100 % within 4 hours of electrolysis. The highest value of CE% 25.27% was obtained at the lowest value of current density (10 mA/cm^2). The maximum removal effectiveness of phenol and any other organic byproducts with SnO$_2$-Sb$_2$O$_3$ electrode revealed that the presence of Sb$_2$O$_3$ with SnO$_2$ enhanced the decomposition of organics.

LITERATURE CITED

1. Lee, C.H., Lee, E.S., Lim, Y.K., Park, K.H., Park, H.D. & Lim, D.S. (2017). Enhanced electrochemical oxidation of phenol by boron-doped diamond nanowire electrode. *RSC Adv*. 7(11), 6229–6235. DOI: 10.1039/c6ra26287b.

2. Mohammed, W.T. & Abdullah, S.M. (2008). Kinetic Study on Catalytic Wet Air Oxidation of Phenol in a Trickle Bed Reactor. *Iraqi J. Chem. Petroleum Engin.* 9(2), 17–23.

3. T. Alnasrawy, S.Y., Alkindi, G. & M. Albayati, T. (2021). Removal of high concentration phenol from aqueous solutions by electrochemical technique. *Engin. Technol. J*. 39(2A), 189–195. DOI: 10.30684/etj.v39i2a.1705.

4. Thwaini, H.H. & Salman, R.H. (2023). Phenol removal by electro-Fenton process using a 3D electrode with iron foam as particles and carbon fibre modified with graphene. *J. Electrochem. Sci. Engin.* 13(3), 537–551. DOI: 10.5599/jese.1806.

5. Ibrahim, H.M. & Salman, R.H. (2022). Study the Optimization of Petroleum Refinery Wastewater Treatment by Successive Electrocoagulation and Electro-oxidation Systems. *Iraqi J. Chem. Petroleum Engin*. 23(1), 31–41. DOI: 10.31699/IJCPE.2022.1.5.

6. Yang, W. (2019). Electrochemical advanced oxidation processes for emerging organic contaminants removal with graphene-based modified carbon felt electrode. Ph. D. Dissertation.

7. Mohammadi, S., Kargari, A., Sanaeepur, H., Abbassian, K., Najafi, A. & Mofarrah, E. (2015). Phenol removal from industrial wastewaters: a short review. *Desalination Water Treat*. 53(8), 2215–2234. DOI: 10.1080/19443994.2014.883327.

8. Naser, G.F., Mohammed, T.J. & Abbar, A.H. (2021). Treatment of Al-Muthanna Petroleum Refinery Wastewater by Electrocoagulation Using a Tubular batch Electrochemical Reactor. IOP Conf. Ser. Earth Environ. Sci. DOI: 10.1088/1755-1315/779/1/012094.

9. Thwaini, H.H. & Salman, R.H. (2023). Modification of Electro-Fenton Process with Granular Activated Carbon for Phenol Degradation – Optimization by Response Surface Methodology. *J. Ecol. Engin.* 24(9), 92–104. DOI: 10.12911/22998993/168411.

10. Steiner, M.G. (2017). Photocatalytic Decomposition of Phenol under Visible and UV Light Utilizing Titanium Dioxide Based Catalysts. New Hampshire.

11. Víctor-Ortega, M.D., Ochando-Pulido, J.M. & Martínez-Ferez, A. (2016). Performance and modeling of continuous ion exchange processes for phenols recovery from olive mill wastewater. *Proc. Safety Environ. Protec*. 100, 242–251. DOI: 10.1016/j.psep.2016.01.017.

12. Divya, N., Sreerag, A.V., Yadukrishna Joseph, T. & Soloman, P.A. (2021). A study on electrochemical oxidationof phenol for wastewater remediation. *IOP Conf. Ser. Mater. Sci. Eng*. 1114(1), 012073. DOI: 10.1088/1757-899x/1114/1/012073.

13. Adil Sabbar, H. (2019). Adsorption of Phenol from Aqueous Solution using Paper Waste. *Iraqi J. Chem. Petrol. Engin*. 20(1), 23–29. DOI: 10.31699/ijcpe.2019.1.4.

14. Ang, W.L., McHugh, P.J. & Symes, M.D. (2022). Sonoelectrochemical processes for the degradation of persistent organic pollutants. *Chem. Engin. J*. 444, 136573. DOI: 10.1016/j.cej.2022.136573.

15. Thokchom, B., Pandit, A.B., Qiu, P., Park, B., Choi, J. & Khim, J. (2015). A review on sonoelectrochemical technology as an upcoming alternative for pollutant degradation. *Ultrason Sonochem*. 27, 210–234. DOI: 10.1016/j.ultsonch.2015.05.015.

16. Symes, D. (2011). Sonoelectrochemical (20 Khz) Production of Hydrogen from Aqueous Solutions. M. Sc. Thesis, The University of Birmingham.

17. Zhang, M., Zhang, Z., Liu, S., Peng, Y., Chen, J. & Yoo Ki, S. (2020). Ultrasound-assisted electrochemical treatment for phenolic wastewater. Ultrason Sonochem. DOI: 10.1016/j.ultsonch.2020.105058.

18. Yaqub, A. & Ajab, H. (2013). Applications of sonoelectrochemistry in wastewater treatment system. *Rev. Chem. Engin*. 29(2), 123–130. DOI: 10.1515/revce-2012-0017.

19. Kim, K., Cho, E., Thokchom, B., Cui, M., Jang, M. & Khim, J. (2015). Synergistic sonoelectrochemical removal of substituted phenols: Implications of ultrasonic parameters and physicochemical properties. *Ultrason Sonochem*. 24, 172–177. DOI: 10.1016/j.ultsonch.2014.11.004.

20. Salman, R.H. & Abbar, A.H. (2023). Optimization of a combined electrocoagulation-electro-oxidation process for the treatment of Al-Basra Majnoon Oil field wastewater: Adopting a new strategy. *Chem. Engin. Processing - Process Intensific*. DOI: 10.1016/j.cep.2022.109227.

21. Nikravesh, B., Shomalnasab, A., Nayyer, A., Aghababaei, N., Zarebi, R. & Ghanbari, F. (2020). UV/Chlorine process for dye degradation in aqueous solution: Mechanism, affecting factors and toxicity evaluation for textile wastewater. *J. Environ. Chem. Eng*. DOI: 10.1016/j.jece.2020.104244.

22. Santos, D., Lopes, A., Pacheco, M.J., Gomes, A. & Ciríaco, L. (2014). The Oxygen Evolution Reaction at Sn-Sb Oxide

Anodes: Influence of the Oxide Preparation Mode. *J. Electrochem. Soc*. 161(9), H564–H572. DOI: 10.1149/2.1031409jes.

23. Feng, Y.J. & Li, X.Y. (2003). Electro-catalytic oxidation of phenol on several metal-oxide electrodes in aqueous solution. *Water Res*. 37(10), 2399–2407. DOI: 10.1016/S0043-1354(03)00026-5.

24. Benchettara, A., Sidoumou, M., Mehdaoui, R., Zarrouk, A. & Benchettara, A. (2019). Electrocatalytic oxidation of paraacetylaminophenol on a graphite electrode modified with iron oxides. *Portugaliae Electrochimica Acta*. 37(6), 383–391. DOI: 10.4152/pea.201906383.

25. Nader, H.J. (2022). Electro-Oxidation of Organic Pollutants in Petroleum Refineries Effluent. M. Sc. Thesis, Al-Nahrain University.

26. Abbas, R.N. & Abbas, A.S. (2022). Kinetics and Energetic Parameters Study of Phenol Removal from Aqueous Solution by Electro-Fenton Advanced Oxidation Using Modified Electrodes with PbO2 and Graphene. *Iraqi J. Chem. Petrol. Engin*. 23(2), 1–8. DOI: 10.31699/ijcpe.2022.2.1.

27. Lv, J., Feng, Y., Liu, J., Qu, Y. & Cui, F. (2013). Comparison of electrocatalytic characterization of boron-doped diamond and SnO2 electrodes. *Appl. Surf. Sci*. 283, 900–905. DOI: 10.1016/j.apsusc.2013.07.040.

28. Subba Rao, A.N. & Venkatarangaiah, V.T. (2014). Metal oxide-coated anodes in wastewater treatment. *Environ. Sci. Pollut. Res*. 21(5), 3197–3217. DOI: 10.1007/s11356-013-2313-6.

29. Zhu, K., Zhang, W., Wang, H. & Xiao, Z. (2008). Electro-catalytic degradation of phenol organics with SnO2-Sb2O3/Ti electrodes. *Clean (Weinh)*. 36(1), 97–102. DOI: 10.1002/clen.200700037.

30. Massa, A., Hernández, S., Ansaloni, S., Castellino, M., Russo, N. & Fino, D. (2018). Enhanced electrochemical oxidation of phenol over manganese oxides under mild wet air oxidation conditions. *Electrochim Acta*. 273, 53–62. DOI: 10.1016/j.electacta.2018.03.178.

31. Santos, I.D. Gabriel, S.B. Afonso, J.C. & Dutra, A.J.B. (2011). Preparation and characterization of Ti/SnO2-Sb electrode by pechini's method for phenol oxidation. *Mater. Res.* 14(3), 408–416.

32. Xu, L., Li, M. & Xu, W. (2015). Preparation and characterization of Ti/SnO2-Sb electrode with copper nanorods for AR 73 removal. *Electrochim. Acta*. 166, 64–72. DOI: 10.1016/j.electacta.2015.02.233.

33. Liu, J. & Feng, Y. (2009). Investigation on the electro-catalytic characteristics of SnO2 electrodes with nanocoating prepared by electrodeposition method. *Sci. in China, Series E: Technol. Sci*. 52(6), 1799–1803. DOI: 10.1007/s11431-009-0110-8.

34. Nsaif, H.J. & Majeed, N.S. (2024). Modified Graphite with Tin Oxide as a Promising Electrode for Reduction of Organic Pollutants from Wastewater by Sonoelectrochemical Oxidation. *Ecol. Engin. Environ. Technol*. 25(1), 307–320. DOI: 10.12912/27197050/175437.

35. Chang, S.T., Leu, I.C. & Hon, M.H. (2002). Preparation and characterization of nanostructured tin oxide films by electrochemical deposition. Electrochemical and Solid-State Letters. DOI: 10.1149/1.1485808.

36. Abbas, R.N. & Abbas, A.S. (2022). The Taguchi Approach in Studying and Optimizing the Electro-Fenton Oxidation to Reduce Organic Contaminants in Refinery Wastewater Using Novel Electrodes.

37. Ahmed, Y.A. & Salman R.H. (2023). Synthesis of Mn-Co-Ni Composite Electrode by Anodic and Cathodic Electrodeposition for Indirect Electro-oxidation of Phenol: Optimization of the Removal by Response Surface Methodology. *Ecol. Engin. Environ. Technol*. 24, 107–119. DOI: 10.12912/27197050/171626.

38. Kötz, R., Stucki, S., Carcer, B. (1991). Electrochemical waste water treatment using high overvoltage anodes. Part I: Physical and electrochemical properties of SnO2, anodes.

39. Zhang, X., Liang, H. & Gan, F. (2006). Novel Anion Exchange Method for Exact Antimony Doping Control of Stannic Oxide Nanocrystal Powder. *J. Amer. Ceramic. Soc*. 89(3), 792–798. DOI: 10.1111/j.1551-2916.2005.00793.x.

40. Yang, X., Zou, R., Huo, F., Cai, D. & Xiao, D. (2009). Preparation and characterization of Ti/SnO2-Sb2O3-Nb2O5/PbO2 thin film as electrode material for the degradation of phenol. *J. Hazard Mater*. 164(1), 367–373. DOI: 10.1016/j.jhazmat.2008.08.010.

41. Pu, Y., Zhao, F., Chen, Y., Lin, X., Yin, H. & Tang, X. (2023). Enhanced Electrocatalytic Oxidation of Phenol by SnO2-Sb2O3/GAC Particle Electrodes in a Three-Dimensional Electrochemical Oxidation System. Water (Switzerland). DOI: 10.3390/w15101844.

42. Khan, H., Yerramilli, A.S., D'Oliveira, A., Alford, T.L. Boffito, D.C. & Patience, G.S. (2020). Experimental methods in chemical engineering: X-ray diffraction spectroscopy—XRD. *Canadian J. Chem. Engin*. 98(6), 1255–1266. DOI: 10.1002/cjce.23747.

43. Vicent, F., Morallo´N,E. Quijada, C.L. Va´Zquez, J. Aldaz, A. & Cases, F. (1998). Characterization and stability of doped SnO2 anodes. *J. Appl. Electrochem*. 28(6), 607–612. DOI: 10.1023/A:1003250118996.

44. Ciríaco, L., Santos, D., Pacheco, M.J. & Lopes, A. (2011). Anodic oxidation of organic pollutants on a Ti/SnO2-Sb 2O4 anode. *J. Appl. Electrochem*. 41(5), 577–587. DOI: 10.1007/s10800-011-0266-3.

45. Li, M., Feng, C., Hu, W., Zhang, Z. & Sugiura, N. (2009). Electrochemical degradation of phenol using electrodes of Ti/RuO2-Pt and Ti/IrO2-Pt. *J. Hazard. Mater*. 162(1), 455–462. DOI: 10.1016/j.jhazmat.2008.05.063.

46. Ren, Y., Wu, Z., Ondruschka, B., Braeutigam, P., Franke, M., Nehring, H. & Hampel, U. (2011). Oxidation of Phenol by Microbubble-Assisted Microelectrolysis. *Chem. Eng. Technol*. 34(5), 699–706. DOI: 10.1002/ceat.201000534.

47. Ren, Y.Z., Wu, Z.L., Franke, M., Braeutigam, P., Ondruschka, B., Comeskey, D.J. & King, P.M. (2013). Sono-electrochemical degradation of phenol in aqueous solutions. *Ultrason Sonochem.* 20(2), 715–721.

48. Neppolian, B., Jung, H., Choi, H., Lee, J.H. & Kang, J.-W. (2002). Sonolytic degradation of methyl tert-butyl ether: the role of coupled fenton process and persulphate ion. *Water Res*. 36(19), 4699–4708. DOI: 10.1016/S0043-1354(02)00211-7.

49. Afsharnia, M., Biglari, H., Rasouli, S.S., Karimi, A. & Kianmehr, M. (2018). Sono-electrocoagulation of fresh leachate from municipal solid waste; Simultaneous applying of iron and copper electrodes. *Int. J. Electrochem. Sci*. 13(1), 472–484. DOI: 10.20964/2018.01.22.

50. Esclapez, M.D., Tudela, I., Díez-García, M.I., Sáez, V., Rehorek, A., Bonete, P. & González-García, J. (2012). Towards the complete dechlorination of chloroacetic acids in water by sonoelectrochemical methods: Effect of the anodic material on the degradation of trichloroacetic acid and its by-products. *Chem. Engin. J*. 197, 231–241. DOI: 10.1016/j.cej.2012.05.031.

51. Veitch, N.C. (2004). Horseradish peroxidase: A modern view of a classic enzyme. *Phytochem*. 65(3), 249–259. DOI: 10.1016/j.phytochem.2003.10.022.

52. Savic, S., Petrovic, S., Petronijevic, stud M. & Petronijevic, Z. (2017). pH and Temperature Influence on Phenol Removal from Water by Horseradish Peroxidase. *Internat. Sci. J. "Mach. Technol. Mater."* (10), 494–496.

53. Abbas, Z.I. & Abbas, A.S. (2021). Optimization of the electro-fenton process for cod reduction from refinery wastewater. *Environ. Eng. Manag. J*. 19(11), 2029–2037. DOI: 10.30638/eemj.2020.192.

54. Ahmed, Y.A. & Salman, R.H. (2023). Simultaneous electrodeposition of multicomponent of Mn–Co–Ni oxides electrodes for phenol removal by anodic oxidation. *Case Studies Chem. Environ. Engin. 8(10038).* DOI: 10.1016/j.cscee.2023.100386.

55. Nurhayati, E., Juang, Y. & Huang, C. (2017). The kinetics, current efficiency, and power consumption of electrochemical dye decolorization by BD-NCD film electrode. AIP Conf Proc. DOI: 10.1063/1.4985519.

56. Abbas, R.N. (2022). Advanced Oxidation of Organic Pollutants in Refinery Wastewater Over Carbon Fiber Electrode. Ph.D. Thesis, University of Baghdad / College of Engineering.

57. Abbas, Z.N. & Abbar, A.H. (2020). Application of response surface methodology for optimization of phenol removal from a simulated wastewater using rotating tubular packed bed electrochemical reactor. *Egypt J. Chem*. 63(10), 3925–3936. DOI: 10.21608/EJCHEM.2020.26727.2547.